HHS Public Access

Author manuscript

Nat Biotechnol. Author manuscript; available in PMC 2018 May 06.

Published in final edited form as:

Nat Biotechnol. 2017 December ; 35(12): 1188–1195. doi:10.1038/nbt.4004.

Generation of TCRs of higher affinity by antigen-driven differentiation of progenitor T cells *in vitro*

Thomas M. Schmitt[1], **David H. Aggen**[2], **Kumiko Ishida-Tsubota**[1], **Sebastian Ochsenreither**[3], **David M. Kranz**[2], and **Philip D. Greenberg**[1,4]

[1]Fred Hutchinson Cancer Research Center, Seattle, Washington 98109

[2]Department of Biochemistry, University of Illinois at Urbana-Champaign, Urbana, Illinois, 61801

[3]Department of Hematology, Oncology, and Tumor immunology, Charité Campus Benjamin Franklin, Berlin, Germany

[4]Departments of Immunology and Medicine, University of Washington, Seattle, Washington 98195

Abstract

Many promising targets for T cell-based cancer immunotherapies are self-antigens. During thymic selection, T cells bearing TCRs with high affinity for self-antigen are eliminated. The affinity of the remaining low avidity TCRs can be improved to increase their anti-tumor efficacy, but conventional saturation mutagenesis approaches are labor intense and the resulting TCRs may be cross-reactive. Here we report an *in vitro* T cell maturation and selection system on antigen-expressing feeder cells for developing high affinity antigen-specific TCRs, which takes advantage of natural *Tcrb* gene rearrangement to generate diversity in the length and composition of CDR3β. *In vitro* differentiation of progenitors transduced with a known *Tcra* in the presence of antigen drives differentiation of cells with a distinct agonist-selected phenotype. These cells are then purified to generate TCRβ chain libraries pre-enriched for target antigen-specificity. Several TCRβ chains were identified that paired with a transgenic TCRα chain to produce a TCR with higher affinity for target antigen compared to the parental TCR.

Introduction

Adoptive T cell immunotherapy with genetically engineered T cells has shown promise in multiple trials in which an antigen receptor of sufficient affinity was used to target a tumor-associated antigen, including antibody-based chimeric receptors[1–3] and high affinity

Authorship Contributions

T.M.S. conceptualized, designed and performed the research, interpreted results and wrote the manuscript, D.H.A. contributed to experimental design and developed the 3D-PYY TCR, K.I. performed and optimized experiments, S.O. contributed to experimental design, D.M.K. designed experiments and interpreted results, and P.D.G designed the experiments, assisted in writing the manuscript, and supervised the study.

Competing Financial Interests Statement

P.D.G. is a co-founder of Juno therapeutics, which is developing T cell based immunotherapies including TCR gene therapy. P.D.G. and T.M.S. are co-inventors on a patent application covering the technology described here.

TCRs[4–8]. However, isolating an effective TCR within the affinity limits imposed by central tolerance remains a substantive roadblock to implementing this approach for the diversity of malignancies in which candidate intracellular self/tumor antigens have been identified[9,10]. Therefore, enhancing the affinity of tumor-specific TCRs beyond the limits of negative selection represents a strategy for creating TCR reagents that have greater potential for achieving tumor eradication, and may be essential for tumors that commonly downregulate MHC class I and thus present limited amounts of the targeted antigen[11].

Methods have been developed to enhance the affinity of TCRs intended for use in TCR gene therapy[10,12–14]. These approaches generally employ saturation mutagenesis targeting the complementarity determining regions (CDRs) that interact predominantly with peptide (CDR3) and/or MHC (CDR1/2)[15]. Mutations in CDR1 or CDR2 theoretically pose a greater risk in the clinic because changes to MHC contact residues can increase TCR affinity for MHC independent of peptide, reducing specificity/selectivity for the cognate peptide antigen[16,17]. CDR1/2 mutations can also alter the docking geometry of the TCR/MHC interaction[18], further increasing risk for cross-reactivity. This notion was highlighted in a recent clinical trial, in which T cells expressing an enhanced affinity TCR containing CDR2 mutations mediated rapid and fatal toxicity from unpredicted cross-reactivity with a nonamer epitope from a self-antigen expressed in the heart, despite being disparate at 4/7 non-anchor residues[19,20]. Although limiting mutations to the CDR3 region may reduce unpredicted cross-reactivities *in vivo*, current methodologies targeting specific CDR3 residues for amino acid substitution generally yield libraries with diversity constrained by the unaltered length of the parental CDR3 sequence. By contrast, the natural process of diversity generation in the thymus employs recombination activating gene (RAG)-mediated TCR gene rearrangements to generate highly diverse CDR3s varying in length as well as amino acid composition. Therefore, greater CDR3 diversity with retention of specificity might be accessed by harnessing the V(D)J recombination machinery active during T cell development.

TCR gene rearrangement begins at the earliest stages of murine T cell development, prior to CD4 and CD8 expression, at the loci that encode the TCRβ, TCRγ and TCRδ chains. Rearrangement at the *Tcra* locus is restricted to the CD4/CD8 double positive (DP) stage, which occurs later. This delayed *Tcra* gene rearrangement plays a central role in dictating γδ versus αβ T cell fate, which is determined by the strength of TCR signals at the $CD4^{-}CD8^{-}CD44^{-}CD25^{+}$ double-negative3 (DN3) stage. A functional TCRβ chain paired with the invariant pre-Tα chain provides a weak signal that promotes αβ lineage commitment (referred to as β-selection) [21]; rearrangement and expression of TCRγ and TCRδ chains can lead to stronger signals that drive γδ lineage commitment[22].

In most transgenic mice expressing an αβTCR, TCRα expression is not delayed, and as a result a population of mature $TCR\alpha\beta^{+}$ DN T cells are often found in the thymus and periphery, which are thought to represent 'γδ wanna-be' cells that develop aberrantly as a result of strong signals delivered through the transgenic αβTCR at the DN3 stage[23,24]. This population does not develop when the transgenic TCRα is expressed only after β-selection[25], and is more pronounced in transgenic mice expressing a TCR specific for a self-antigen (e.g., male mice with a TCR specific for male HY antigen have substantially more

TCRαβ$^+$ DN T cells compared to female littermates[24,26]). This suggests that in TCR-transgenic animals, the TCRαβ$^+$ DN T cell population represents a distinct population of agonist-selected T cells, and that stronger agonist signals prior to β-selection promote the development of this lineage.

These findings suggest that TCR affinity could be enhanced by recapitulating this process *in vitro* using hematopoietic progenitor cells (HPCs) that ectopically express only the TCRα chain from a target antigen-specific TCR prior to β-selection. HPCs can be induced to expand and differentiate into T lineage cells on OP9-DL1 cells[27,28], generating a large pool of progenitor T cells with unique, naturally occurring *Tcrb* gene rearrangements. We hypothesized that, when these progenitors are differentiated in the presence of cognate antigen, those expressing a TCRβ chain that confers high affinity for the target antigen when paired with the TCRα chain will be diverted to a DN TCRαβ$^+$ lineage. These agonist-selected cells could then be isolated to identify endogenous TCRβ chains that produce the highest affinity antigen-specific αβTCRs.

Results

Development of phenotypically mature DN TCRαβ$^+$ T cells

To determine if progenitor thymocytes from mice expressing an αβ–TCR also differentiate into DN TCRαβ$^+$ cells *in vitro* in response to cognate antigen, TCRαβ$^-$CD4$^-$CD8$^-$CD117$^+$CD44$^+$ (DN1/DN2) progenitor thymocytes were sorted from ovalbumin (OVA)-specific TCR-transgenic OT1 mice and cultured on OP9-DL1 cells expressing H-2K^b and H-2D^b (OP9-K^{b}D^{b}DL1) in the absence of peptide, or with increasing concentrations of the OVA peptide SIINFEKL. In the absence of peptide, DP T cells were detected at day 16, and constituted a major fraction of the cell culture by day 20, as previously reported[28,29]. However, development and/or survival of DP T cells was diminished by even very low concentrations of SIINFEKL peptide (0.0001uM), and DP cells were completely absent from cultures containing 0.01uM or more of peptide (Fig. 1a), suggesting DP cells fail to develop or are negatively selected by strong agonist signaling in OP9-K^{b}D^{b}DL1 cultures, as observed *in vivo*[30]. The majority of cells on day 5 displayed an immature TCRβ$^-$ CD24$^+$ phenotype (Fig. 1b), but by day 16 most DN cells from all culture conditions expressed TCRβ, with more TCRβ$^+$CD24$^-$ cells detected at the higher peptide concentrations. By day 20, ~60% of all DN cells were TCRβ$^+$CD24$^-$ from cultures containing 0.01μM or 1.0μM peptide, whereas in cultures that received no or very low concentration (0.0001μM peptide only ~20% of DNs were TCRβ$^+$CD24$^-$, and ~50% were TCRβ$^-$, and likely of NK lineage (Fig. 1b,c). Furthermore, DN TCRβ$^+$ cells that developed in response to high peptide concentrations expressed higher levels of cell surface TCRβ, consistent with a more mature phenotype (Fig. 1c). High concentrations of SIINFEKL, but not the positive-selecting antagonist peptide EIINFEKL (E1)[30], led to increased absolute numbers of DN TCRβ$^+$ T cells (Fig. 1d), indicating more avid TCR signaling enhances development of this population. This effect appears to plateau at very high concentrations of peptide above 0.1μM. To confirm that TCRαβ$^+$ DN cells observed in these cultures did not develop by passing through a DP stage, pre-selection CD69$^-$ DP T cells were sorted from the thymus of wild type C57BL/6 (B6) or OT1 TCR-transgenic mice and cultured on OP9-

K^bD^bDL1 cells in the presence or absence of SIINFEKL peptide (Supplementary Fig. 1). Whereas B6 DP cells were not impacted by the presence of SIINFEKL peptide, OT1 DP thymocytes cultured in the presence of SIINFEKL exhibited the hallmarks of negative selection, including CD4/CD8 co-receptor down-modulation and loss of cellularity[31], and DN $TCR\beta^+$ cells were not detected.

Generation of agonist-selected TCRβ chains in vitro

We sorted DN1 and DN2 thymocytes ($TCR\alpha\beta^-CD4^-CD8^-CD117^+CD44^+$) from B6 mice and retrovirally transduced with a vector containing the extracellular domain of human CD2 (hCD2) to track transduced cells, and the TCRα chain 3D-PYYα from a previously described H-$2D^b$-restricted TRBV4 (Vβ10)/TRAV9-1 TCR specific for the WT1 tumor antigen RMFPNAPYL epitope and affinity-enhanced by saturation mutagenesis of CDR3α[32,33]. Transduced progenitor thymocytes were cultured on OP9-K^bD^bDL1 cells in the presence or absence of 1.0mM RMFPNAPYL for 14 days. DN cells within the untransduced hCD2 negative fraction contained <2% $TCR\alpha\beta^+$ cells, regardless of the presence of the WT1 peptide in the culture. In contrast, the DN fraction from the transduced $hCD2^+$ population contained 6.8% $TCR\beta^+$ cells on day 16 in the absence of peptide, and $TCR\alpha\beta^+$ cells increased to 16.6% if 1μM WT1 peptide was added (Fig. 2a).

We expected a fraction of these cells to recognize the WT1 peptide, but could not detect WT1 $tetramer^+$ DN cells, either due to lack of CD8 expression, lower TCR surface levels, or low frequency. Therefore, we generated a library of TCRβ chains from the DN $TCR\beta^+$ population that develops from 3D-PYYα-transduced HPCs cultured on OP9-K^bD^bDL1 with peptide, to identify TCRβ chains that confer WT1 tetramer binding when paired with 3D-PYYα. Sequences from >30 clones were analyzed, and the top four TCRβ chains by frequency advanced for further study. All these clones had CDR3β sequences that shared multiple residues with the parental 3Dβ chain (Fig. 2c), with Clone#1 almost identical to the original 3Dβ (Fig. 2c and Supplementary Fig. 3). The four candidate TCRβ chains were retrovirally transduced into $58^{-/-}$3D-PYYα cells and analyzed by flow cytometry (Fig. 2d). All four TCRs bound tetramer, although clone#4, which exhibited the weakest homology to the original 3D CDR3β bound tetramer at substantially lower levels and was not analyzed further.

The approximate relative affinity for tetramer of two of the three candidate TCRβ chains when paired with 3D-PYYα, was higher than the original 3Dβ, with Clone#1 having >3 fold higher affinity (Fig. 3a and Methods). To more accurately compare tetramer staining of 3D-PYYα Clone#1 TCRβ versus the original 3Dβ, Clone#1 was codon-optimized such that the only sequence differences between the original 3Dβ and Clone#1 were in the CDR3 region. As expected, transduced T cells expressing the Clone#1 TCRβ chain at similar levels to the parental 3Dβ chain exhibited enhanced tetramer staining (Fig. 3b). Clone#1 transduced $58^{-/-}$3D-PYYα cells were stained with a panel of H-$2D^b$-tetramers containing alternative peptides, and no staining could be detected using other peptide/H-$2D^b$ tetramers (Fig. 3c), suggesting the increased affinity observed for these receptors is not the result of increased affinity for MHC alone.

TCRβ+ DN cells develop in the thymus of TCRα retrogenic mice

WT1 is expressed in the thymus[34,35], and we wanted to determine if a similar selection process would occur during thymic development *in vivo* in mice. In mice, agonist-selected T cells may accumulate throughout the life of the animal, allowing a broader repertoire of TCRs reactive to this self-antigen to be assessed. Therefore, we generated TCRα retrogenic mice by transferring 3D-PYYα-transduced hematopoietic stem cells (HSCs) into irradiated recipient mice[36]. A substantially increased population of DN TCRβ$^+$ cells was detected among 3D-PYYα-transduced thymocytes and splenocytes compared to untransduced controls (Fig. 4a). Furthermore, these thymocytes contained an increased proportion of T cells expressing the Vβ10 gene utilized by the original 3Dβ (Fig. 4a), suggesting at least some DN TCRβ$^+$ cells might be specific for the same WT1 antigen.

We generated Vβ10-Cβ1 and Vβ10-Cβ2 libraries from DN TCRαβ$^+$ cells (Fig. 4b) enriched for binding to WT1 tetramer (Supplementary Fig. 2 and Methods) and recovered TCRβ chains (Fig. 4c). Three dominant clones were analyzed (Fig. 4d), with Thyβ#1 showing enhanced tetramer binding compared to 3Dβ, while Thyβ#2 and Thyβ#3 appeared to have similar or slightly lower affinity compared to 3Dβ, respectively. TCR 3D-PYYα-Thyβ1 exhibited enhanced affinity compared to T cells expressing 3D-PYYα-3Dβ (Fig. 4e), and enhanced IFNγ production in response to peptide-pulsed target cells (Fig. 4f). Thyβ#1 differs from the original 3Dβ chain by only one amino acid at position 108 (Fig. 4b), which is one of the two positions for which Clone#1 from the OP9-DL1-derived TCRβ library screen differed from 3Dβ (Fig. 2b, and Supplementary Fig. 3), suggesting the proline at this position in the parental 3Dβ either does not optimally contribute or has a negative impact on peptide binding.

To assess the *in vivo* safety of the highest affinity murine TCRs generated, P14 CD8$^+$ T cells were transduced to express codon-optimized, P2A-linked TCR chains (3Dαβ or 3D-PYYα paired with either 3Dβ, *in vitro*-derived Vβ10 clone#1, or Thyβ#1). We injected the TCR-transduced T cells into C57BL/6 mice, and assessed autoimmunity, including weight loss and transgenic T cell expansion. Somewhat decreased numbers were observed for T cells transduced with the enhanced affinity Vβ chains at the late (day 126) time point, perhaps reflecting a moderate increase in peripheral tolerance and/or deletion [37]. Otherwise, no toxicities or differences were observed between these WT1-specific T cells (Supplementary Fig. 4).

To examine the full TCRβ repertoire of agonist-selected DN TCRαβ+ cells, we analyzed DN TCRαβ$^+$ thymocytes from 3D-PYYα retrogenic mice by high-throughput sequencing and repertoire analysis[38] (Supplementary Fig. 5). 141,113 unique TCRβ chain sequences were identified from 1,486,250 reads representing 288,000 sorted cells. The clonality was 0.05, with the most frequent clone representing 0.04% of the total, indicating this lineage-diverted population is highly diverse with limited clonal expansion. Only a small percentage of the TCRβ repertoire expressed Vβ10 (TRBV4), and substantial expansion of TRBV17$^+$ cells was observed compared to total C57BL/6 thymocytes, with 9 of the top 10 most common TCRβ sequences utilizing this Vβ-gene. However, screening of diverse RACE PCR-based libraries revealed only Vβ10 TCRβ chains were reactive with WT1 (data not shown). Therefore, TCRs incorporating Vβ17 chains are more likely specific for thymus-

expressed antigens other than WT1. Thus, restricting TCRβ chain libraries to the parental TCRβ gene should not only increase the frequency of TCRs that bind the target antigen but also minimize isolation of TCRs with alternative specificities.

Generation of human agonist-selected TCRβ chains in vitro

To extend the approach to human specificities, cord blood-derived $CD34^+$ HPCs were selected and transduced to express the P2A-linked TCRαβ chains of a high affinity HLA-A2-restricted human TCR specific for $WT1_{37\text{-}45}$ ($WT1_{37}$αβ) and cultured on OP9-DL1 cells expressing HLA-A2 (OP9-A2-DL1) in the presence or absence of WT1 peptide (Supplementary Fig. 6). After 22 days, human HPC transduced with $WT1_{37}$αβ and cultured on OP9-A2-DL1 cells included a substantial population of $CD3^+$ $CD4^-$ $CD27^+$ cells heterogeneous for CD8 (~75% $CD8^-$), consistent with γδ lineage cells[41, 42], which were mostly absent from untransduced controls (Supplementary Fig. 6). Addition of cognate WT1 peptide to the cultures increased the proportion of these cells (from 29.6% to 40.2%), suggesting enrichment for agonist-selected T cells.

Human $CD34^+$ HPCs were then transduced to express only the TCRα chain of TCR $WT1_{37}$ ($WT1_{37}$α), and cultured with OP9-A2-DL1 cells in the presence of cognate WT1 peptide. Compared to untransduced controls, $WT1_{37}$α expressing progenitors contained a greater proportion of $CD3^+$ $CD27^+$ cells, which included a unique population of $TCR\beta^+$ $CD8^-$ cells within the transduced $CD3^+$ $CD27^+$ subset (Fig. 5a,b). We sorted $CD3^+$ $TCR\beta^+$ $CD27^+$ DN and $CD3^+$ $TCR\beta^+$ $CD8^+$ $CD27^{hi}$ cells as the populations most likely to contain agonist-selected cells, and generated TCRβ libraries. As the parental TCRβ chain utilizes TRBV19 (Vβ17), we generated Vβ17-restricted Cβ1 and Cβ2 libraries, as well as separate more diverse RACE PCR-derived libraries. The TCRβ libraries were transduced into the $CD8^-$ T cell line H9 previously transduced to express $WT1_{37}$α (H9.$WT1_{37}$α), and Vβ17 library-transduced cells were sorted for Vβ17 expression (Fig. 5c). We enriched for WT1 tetramer-reactive cells and detected a range of tetramer reactivity post-enrichment, suggestive of an enriched pool of TCRβ chains with a range of affinities for HLA-A2/WT1 (Fig.5c). 26 TCRβ chains were detected multiple times, and these were coexpressed in the $CD8^-$ TCRαβ-deficient Jurkat76 cell line with $WT1_{37}$α. 11 of the 26 TCRβ chains bound WT1 tetramer independent of CD8 when paired with $WT1_{37}$α (Supplementary Fig. 7a). This group contained three Vβ families, three Jβ families, and CDR3 regions ranging from 13–16 amino acids (Supplementary Fig. 7a). Vβ17 was utilized by 9 of these 11 TCRs, and 3 $V\beta17^+$ TCRs exhibiting the highest tetramer binding were selected for further study (Fig. 6b). The TCR with the highest apparent affinity, Vβ15#1, was also further analyzed, although TCRs utilizing non-parental Vβ chains would require extensive screening for potential cross-reactivities before being considered for clinical use. Codon-optimized lentiviral constructs (TCRβ-P2A-$WT1_{37}$α) were synthesized for each TCRβ chain, and expressed in Jurkat76 cells (Fig. 6b). All of the selected TCRβ chains exhibited enhanced tetramer binding compared to the wildtype TCRβ chain when paired with $WT1_{37}$α (Fig. 6c). We transduced the TCRs into primary human $CD8^+$ T cells and expanded sorted $tetramer^+$ $CD8^+$ T cells. Each $V\beta17^+$ TCR expressed similar levels of the transgenic Vβ17 chain and all transduced populations expressed similar levels of CD8 (Supplementary Fig. 8a). T cells expressing enhanced affinity TCRs Vβ17#2-P2A-$WT1_{37}$α, Vβ17#3-P2A-

$WT1_{37}\alpha$, and Vβ15#1-P2A-$WT1_{37}\alpha$ exhibited enhanced IFNγ production in response to titrated concentrations of WT1 peptide compared to wild-type Vβ17*wt* $\alpha\beta$ TCR (Fig. 6d), and none of the TCRs produced IFNγ in the absence of peptide (Supplementary fig. 8b). Despite enhanced affinity for $WT1_{37}$ tetramer (Fig. 6b,c), TCR Vβ17#7-P2A- $WT1_{37}\alpha$ displayed a diminished functional response to WT1 peptide. As discrepancies have been previously reported between affinity measured by tetramer binding (which occurs in 3 dimensions) and functional readouts that depend on TCR-peptide/MHC interactions at the 2 dimensional T cell-APC interface[39,40], these results highlight the necessity for functional screening of candidate TCRs in addition to tetramer-based assays. Taken together, these data demonstrate the utility of this approach for isolating enhanced affinity TCRs specific for human tumor/self-antigens.

Discussion

Here we report on a system for efficiently generating and screening diverse CDR3β chains pre-enriched for specific antigen reactivity from which enhanced affinity TCRs can be isolated. This approach takes advantage of the fact that agonist signaling through a mature TCR$\alpha\beta$ complex before the β-selection checkpoint does not result in negative selection, but rather results in T cell differentiation to a distinct DN TCR$\alpha\beta^+$ lineage with similarities to $\gamma\delta$ T cells. Because TCRβ libraries are generated from a population selectively enriched for cells responding to an agonist TCR signal during differentiation, the resulting library requiring analysis for antigen reactivity can be much smaller than the typical saturation mutagenesis libraries commonly used to generate high affinity TCRs [33,41,42].

A major concern for clinical translation of affinity-enhanced TCRs is the risk of off-target T cell activation and autoimmunity. While any modification to the antigen binding domains of a TCR could potentially lead to off-target toxicity, modifications limited to CDR3 are less likely to influence interactions with MHC independent of peptide[43]. V-D-J recombination at the *TRB* locus can produce extensive CDR3β diversity in both length and amino acid composition through differential V-D-J gene segment usage, nucleotide deletions, and non-germline-encoded N- and P- nucleotide additions at the V-D and D-J junctions. As such, this approach has potential for CDR3 diversity, minimizing the need for improving affinity by additional CDR1/2 mutations. Notably, three of the five enhanced affinity human TCRβ chains isolated in this study have a longer CDR3 than the parental TCRβ chain (Fig. 6a and Supplemental Fig. 7).

One limitation of this system is that it is necessarily restricted to the TCRβ chain. However, this approach can be readily coupled with traditional saturation mutagenesis of TCRα CDR3 regions. Indeed, the murine 3Dα-PYY TCR used in our study contains affinity-enhancing mutations in CDR3α, and when paired with the parental 3Dβ, has been shown to exceed the affinity limits imposed by negative selection[32]. The fact that we could isolate TCRs with affinities that surpassed that of the 3D-PYY$\alpha\beta$ TCR affirms that this system can generate TCRs that would normally be excluded from the peripheral T cell repertoire[32].

Tumor-reactive $CD4^+$ T cells can exhibit potent antitumor activity through recognition of tumor-associated MHC-II ligands[44–46], but most solid tumors do not express MHC-II

molecules, limiting the ability of $CD4^+$ T cells to function at the tumor site. However, MHC-I-restricted TCRs with sufficient affinity to bind peptide/MHC and signal independent of a contribution by CD8 can be used to redirect CD4 T cells to recognize MHC-I-presented antigens[47]. Although such TCRs have been naturally isolated[48], most require higher affinity for peptide/MHC-I than is typical for naturally occurring MHC-I-restricted TCRs[47]. The agonist-selected T cells we describe develop in the absence of CD8 (i.e., from DN thymocytes), and may therefore express TCRs more likely to function independent of CD8 in mature T cells. In fact, all the enhanced-affinity human WT1-specific TCRs generated bound peptide/MHC independent of CD8 (Fig. 6b). Thus, one potential application of these enhanced affinity TCRs is for engineering CD4 T cells to recognize and respond to the same antigen on the same tumor target as CD8 T cells [47]. This approach could theoretically provide CD4 T cell help and effector mechanisms to a tumor site in addition to $CD8^+$ effector cells, which would be expected to create more potent and sustained anti-tumor activity [49].

Online Methods

Mice

C57BL/6 (B6) mice were purchased from the Jackson Laboratory, OT1 mice were a gift from M. Bevan (University of Washington, Seattle, WA), and P14 TCR transgenic mice bred on the B6 background were a kind gift from Dr. Murali Krishna-Kaja. All animal research performed for this study was approved under University of Washington Institutional Animal Care and Use Committee protocol 2013-01.

Cell lines

The retroviral packaging line PlatE was obtained from Cell Biolabs (San Diego, CA), The OP9-K^bD^bDL1 cell line was generated by transducing the OP9 cell line with a retroviral construct containing the Dll-1 gene followed by an IRES and H-$2K^b$ (to generate OP9-K^bDL1 cells), and separately transduced with H-$2D^b$. The OP9-K^bD^bDL1-WT1 cell line was also then transduced to express murine WT1. The OP9-A2-DL1 cell line was generated by transducing OP9-K^bDL1 cells with a retroviral construct encoding HLA-A2-IRES-human β2M. The OP9 cells and a retroviral construct containing the Dll1 gene followed by IRES-GFP were obtained from the lab of Juan Carlos Zúñiga-Pflücker. The $58^{-/-}$3D-PYYα cell line was generated by retrovirally tranducing a CD8α/CD8β expressing variant of the TCRα/TCRβ-deficient cell line 58−/−[27,50] with Mig2-3D-PYYα. The H9.$WT1_{37}$α cell line was generated by lentivirally transducing the human T cell line H9 with $WT1_{37}$α-IRES-GFP. The TCRαβ negative Jurkat76 cell line was obtained from David Kranz.

Flow cytometric analysis and cell sorting

Flow cytometric analysis data was collected using a BD Biosciences Canto I or Canto II running BD FACSDiva software, and Flow cytometric cell sorting was performed using a BD Biosciences Aria II running FACSDiva software. Data analysis was performed using FlowJo software (Tree Star, Ashland OR). Initial gating of live cell populations for analysis was performed as indicated in Supplementary Fig. 9. The following antibody clones were used for analysis of murine cell antigens: CD4 (RM4-5), CD8α (53-6.7), TCRβ (H57-597),

CD24 (M1/69), and Vβ10 (B21.5); and of human cell surface antigens: CD2 (RPA-2.10), Vβ17 (E17.SF3.15.13), and CD27 (M-T271). HLA-A2/WT1 and H-2Db/WT1 tetramers were generated by the Immune Monitoring Lab at the Fred Hutchinson Cancer Research Center. The optimal staining concentration for each tetramer was determined empirically by staining mixed positive and negative control T cell lines with titrated concentrations of tetramer and selecting the tetramer concentration yielding the best separation between positive and negative populations.

TCR constructs and plasmids

The murine WT1-specific TCR 3D was isolated from the highest affinity T cell clone that could be detected from immunized B6 mice that was specific for the immunodominant H-2D^b epitope of WT1 RMFPNAPYL ($WT1_{126\text{-}134}$). The Mig2-3D-PYYα construct consists of a codon-optimized enhanced affinity variant of the 3D TCRα chain[32], followed by an IRES and the transmembrane and extracellular domains of human CD2. TCR gene expression is driven by the retroviral LTR. The Retroviral vector Mig-AttR and lentiviral vector pRRLSIN-AttR were generated by cloning the *ccdb* gene flanked by AttR sites (the EcoRV fragment) from the lentiviral vector pLenti (Invitrogen) into the HpaI site of the retroviral vector MigR1[10,51], or ASC_I and Sal-I sites of pRRLSIN.cPPT.MSCV/GFP.WPRE, replacing GFP. The lentiviral vectors pRRLSIN-$WT1_{37}$αβ and pRRLSIN-$WT1_{37}$α were generated from the vector pRRLSIN.cPPT.MSCV/GFP.WPRE by replacing GFP with a cassette encoding pRRLSIN-$WT1_{37}$α or both the TCRα and –β chains of $WT1_{37}$ separated by a P2A element. The vector pRRLSIN.cPPT.MSCV/GFP.WPRE was a kind gift from Richard Morgan.

In vitro T cell differentiation

Thymocytes were isolated from B6 or OT1 mice, depleted of CD4$^+$ and CD8$^+$ cells by magnetic bead separation (Miltenyi Biotec), and sorted for CD117$^+$ CD44$^+$ CD4$^-$ CD8$^-$ double negative 1 and 2 (DN1/2) early progenitor thymocytes. DN1/2 cells were either directly transferred to OP9-DL1 cells, or retrovirally transduced with supernatant from PlatE cells transduced with Mig2-3D-PYYα prior to OP9-DL1 culture. Progenitor thymocytes were cultured in the presence of IL-7 (1ng/ml) and Flt3L (5ng/ml) as previously described[27,50], and cognate antigen (peptide $WT1_{126\text{-}134}$). For human T cell differentiation, CD34$^+$ hematopoietic stem and progenitor cells (HPCs) were purified from cord blood by magnetic bead separation (Miltenyi Biotec), lentivirally transduced, and cultured on OP9-A2-DL1 cells in the presence of human cytokines SCF (20ng/ml), TPO (20ng/ml), IL-7 (10 ng/ml) and Flt3L (5ng/ml) in the presence or absence of peptide $WT1_{37\text{-}45}$ as indicated. The de-identified cord blood samples were provided by Colleen Delaney (Fred Hutchinson Cancer Research Center, Seattle, WA) through a cord blood collection protocol at Swedish Medical Center, Swedish IR 3834S-03/FHCRC IRB #5647, which requires informed consent be obtained from all subjects. Donor PBMCs samples were collected according to the Declaration of Helsinki principles on protocol FHCRC#176 approved by the Fred Hutchinson Cancer Research Center Institutional Review Board. All donors provided written informed consent.

Generation of retrogenic mice

Retrogenic mice were generated as described previously[32,50]. Briefly, bone marrow (BM) cells were isolated from the leg bones of B6 mice, and HPCs were enriched by magnetic cell sorting, using the mouse lineage cell depletion kit from Miltenyi. The HPCs were cultured in media containing IL-3 (20 ng/mL), IL-6 (50 ng/mL), stem cell factor (50 ng/mL), and FLT-3L (5 ng/mL) for 3 days. On the first 2 days after BM isolation, the purified progenitor cells were retrovirally transduced with the 3D-PYYα construct; on the third day the transduced HPCs were injected into sublethally irradiated B6 host mice. No blinding or randomization was performed for these experiments.

Generation and screening of TCRβ chain libraries

RNA was isolated from *In vitro* cultured or retrogenic murine thymocytes or *in vitro*-differentiated human progenitors that were sorted as indicated, and RACE-ready cDNA was generated (SMARTer RACE kit, Clontech). Full-length *Tcrb* genes were PCR amplified using a modified RACE universal primer mix that contains a CACC at the 5′ end or a CACC-containing a murine Vβ10 or human Vβ17 primer paired with a mouse or human Cβ1 or Cβ2 specific reverse primer. The CACC was added to the 5′ end to facilitate directional cloning into the Topo vector pEntr/D-Topo (Invitrogen). Topo reactions were electroporated into Electromax DH10B T1 cells and 50,000–500,000 colonies were recovered. The libraries were then combined and transferred into Mig-AttR (mouse) or pRRLSIN-AttR (human) by Gateway cloning (Invitrogen). $58^{-/-}$3D-PYYα cells (H9.$WT1_{37}$α cells for human libraries) were transduced with the TCRβ retroviral libraries and subjected to multiple rounds of sorting based on high level WT1-specific tetramer staining. Library-derived TCRβ chains were recovered from transduced cells exhibiting the highest level of tetramer staining and analyzed by sequence analysis. Candidate TCRβ chains were expressed in the relevant TCRα-expressing T cell line or co-expressed with TCRα in primary T cells and relative affinity was assessed by staining transduced cells with 2-fold serial dilutions of WT1 tetramer and fitting the MFI values for each positive population to a saturation binding curve by nonlinear regression using GraphPad Prism software. Functional avidity was assessed by stimulating TCR-transduced mouse or human primary $CD8^+$ T cells with murine splenocytes or the human T2 cells pulsed with titrated concentrations of WT1 peptide. Duplicate samples of sort-purified TCR-transduced T cells were incubated 1:1 with APCs pulsed with $WT1_{37}$ peptide at the indicated concentrations for 6 hours in the presence of golgiplug and golgistop (BD biosciences). Cells were then permeabilized, stained with anti-IFNγ antibody, and analyzed by flow cytometry.

Adaptive Biotechnologies ImmunoSEQ assay

A multiplex PCR system was used to amplify CDR3β sequences from DNA samples using 35 forward primers for the Vβ gene segment and 14 reverse primers for the Jβ segment. This approach generates a 60 base-pair fragment capable of identifying the VDJ region spanning each unique CDR3β[32,38,51]. Amplicons were sequenced using the Illumina HiSeq platform and data was analyzed using the ImmunoSEQ analyzer toolset.

Statistics

Statistical data for *in vitro* cellular expansion (figure 1d) and T cell functional assays (IFNγ production in response to peptide) were presented as means ± standard error of mean (s.e.m., denoted as error bars); for figure 1d n=3 cell culture replicates and for IFNγ assays n=2 cell culture replicates. Derived relative K_D values were calculated from binding curves in Graphpad Prism by non-linear regression (one site binding, hyperbola). Error bars represent 95% confidence limits for each calculated K_D value.

Data availability

High-throughput sequencing and repertoire analysis in supplementary figure 5 has been deposited in the ImmuneACCESS database (URL: https://doi.org/10.21417/B7SH0W). Additional source data are available from the corresponding author upon request.

A Life Sciences Reporting Summary for this paper is available.

Supplementary Material

Refer to Web version on PubMed Central for supplementary material.

Acknowledgments

This work was supported by the US National Institutes of Health (NIH) (P01 CA18029-40 P.D.G.; R01 CA033084-32, P.D.G.; NIH CA178844, D.M.K.) and the Guillot Family Fund. T.M.S. is supported by the Jose Carreras International Leukemia Foundation 2013 E.D. Thomas Post-Doctoral Fellowship. We would also like to thank C. Delaney for providing cord blood samples, L. Badenhorst for technical assistance, S. Tan for help with *in vivo* experiments, and N. Duerkopp for administrative assistance.

References

1. Kalos M, et al. T cells with chimeric antigen receptors have potent antitumor effects and can establish memory in patients with advanced Leukemia. Sci Transl Med. 2011; 3:95ra73–95ra73.
2. Porter DL, Levine BL, Kalos M, Bagg A, June CH. Chimeric antigen receptor-modified T cells in chronic lymphoid leukemia. N Engl J Med. 2011; 365:725–733. [PubMed: 21830940]
3. Kochenderfer JN, et al. Eradication of B-lineage cells and regression of lymphoma in a patient treated with autologous T cells genetically engineered to recognize CD19. Blood. 2010; 116:4099–4102. [PubMed: 20668228]
4. Chapuis AG, et al. Transferred WT1-reactive CD8+ T cells can mediate antileukemic activity and persist in post-transplant patients. Sci Transl Med. 2013; 5:174ra27.
5. Chapuis AG, et al. Transferred melanoma-specific CD8+ T cells persist, mediate tumor regression, and acquire central memory phenotype. Proc Natl Acad Sci U S A. 2012; doi: 10.1073/pnas.1113748109
6. Morgan R, et al. Cancer Regression in Patients After Transfer of Genetically Engineered Lymphocytes. Science. 2006; 314:126–129. [PubMed: 16946036]
7. Dudley M, et al. Adoptive cell therapy for patients with metastatic melanoma: evaluation of intensive myeloablative chemoradiation preparative regimens. J Clin Oncol. 2008; 26:5233–5239. [PubMed: 18809613]
8. Robbins PF, et al. Tumor regression in patients with metastatic synovial cell sarcoma and melanoma using genetically engineered lymphocytes reactive with NY-ESO-1. Journal of Clinical Oncology. 2011; 29:917–924. [PubMed: 21282551]
9. Stromnes IM, et al. Abrogation of SRC homology region 2 domain-containing phosphatase 1 in tumor-specific T cells improves efficacy of adoptive immunotherapy by enhancing the effector

function and accumulation of short-lived effector T cells in vivo. The Journal of Immunology. 2012; 189:1812–1825. [PubMed: 22798667]

10. Schmitt TM, Ragnarsson GB, Greenberg PD. T Cell Receptor Gene Therapy for Cancer. Hum Gene Ther. 2009; 20:1240–1248. [PubMed: 19702439]
11. Garrido F, Aptsiauri N, Doorduijn EM, Garcia Lora AM, van Hall T. The urgent need to recover MHC class I in cancers for effective immunotherapy. Curr Opin Immunol. 2016; 39:44–51. [PubMed: 26796069]
12. Udyavar A, Alli R, Nguyen P, Baker L, Geiger TL. Subtle affinity-enhancing mutations in a myelin oligodendrocyte glycoprotein-specific TCR alter specificity and generate new self-reactivity. J Immunol. 2009; 182:4439–4447. [PubMed: 19299745]
13. Zhao Y, et al. High-affinity TCRs generated by phage display provide CD4+ T cells with the ability to recognize and kill tumor cell lines. J Immunol. 2007; 179:5845–5854. [PubMed: 17947658]
14. Richman S, Kranz D. Display, engineering, and applications of antigen-specific T cell receptors. Biomolecular Engineering. 2007; 24:361–373. [PubMed: 17409021]
15. Wucherpfennig KW, Gagnon E, Call MJ, Huseby ES, Call ME. Structural biology of the T-cell receptor: insights into receptor assembly, ligand recognition, and initiation of signaling. Cold Spring Harb Perspect Biol. 2010; 2:a005140. [PubMed: 20452950]
16. Huseby ES, Crawford F, White J, Marrack P, Kappler JW. Interface-disrupting amino acids establish specificity between T cell receptors and complexes of major histocompatibility complex and peptide. Nat Immunol. 2006; 7:1191–1199. [PubMed: 17041605]
17. Stadinski BD, et al. A role for differential variable gene pairing in creating T cell receptors specific for unique major histocompatibility ligands. Immunity. 2011; 35:694–704. [PubMed: 22101158]
18. Wang JH, Reinherz EL. The structural basis of αβ T-lineage immune recognition: TCR docking topologies, mechanotransduction, and co-receptor function. Immunol Rev. 2012; 250:102–119. [PubMed: 23046125]
19. Cameron BJ, et al. Identification of a Titin-derived HLA-A1-presented peptide as a cross-reactive target for engineered MAGE A3-directed T cells. Sci Transl Med. 2013; 5:197ra103–197ra103.
20. Linette GP, et al. Cardiovascular toxicity and titin cross-reactivity of affinity-enhanced T cells in myeloma and melanoma. Blood. 2013; 122:863–871. [PubMed: 23770775]
21. von Boehmer H, et al. Pleiotropic changes controlled by the pre-T-cell receptor. Curr Opin Immunol. 1999; 11:135–142. [PubMed: 10322152]
22. Pennington D, Silva-Santos B, Hayday A. Gammadelta T cell development--having the strength to get there. Curr Opin Immunol. 2005; 17:108–115. [PubMed: 15766668]
23. Terrence K, Pavlovich C, Matechak E, Fowlkes B. Premature expression of T cell receptor (TCR)alphabeta suppresses TCRgammadelta gene rearrangement but permits development of gammadelta lineage T cells. 2000; 192:537–548.
24. Egawa T, Kreslavsky T, Littman D, von Boehmer H. Lineage diversion of T cell receptor transgenic thymocytes revealed by lineage fate mapping. PLoS ONE. 2008; 3:1512.
25. Baldwin TA, Sandau MM, Jameson SC, Hogquist KA. The timing of TCR alpha expression critically influences T cell development and selection. 2005; 202:111–121.
26. von Boehmer H, Kirberg J, Rocha B. An unusual lineage of alpha/beta T cells that contains autoreactive cells. 1991; 174:1001–1008.
27. Schmitt T, Zúñiga-Pflücker J. Induction of T cell development from hematopoietic progenitor cells by delta-like-1 in vitro. Immunity. 2002; 17:749–756. [PubMed: 12479821]
28. Schmitt T, Zúñiga-Pflücker J. T-cell development, doing it in a dish. Immunol Rev. 2006; 209:95. [PubMed: 16448536]
29. Schmitt T, et al. Induction of T cell development and establishment of T cell competence from embryonic stem cells differentiated in vitro. Nat Immunol. 2004; 5:410–417. [PubMed: 15034575]
30. Hogquist K, Jameson S, Bevan M. Strong agonist ligands for the T cell receptor do not mediate positive selection of functional CD8+ T cells. Immunity. 1995; 3:79–86. [PubMed: 7621079]
31. Page DM, Kane LP, Allison JP, Hedrick SM. Two signals are required for negative selection of CD4+CD8+ thymocytes. J Immunol. 1993; 151:1868–1880. [PubMed: 7688388]

32. Schmitt TM, et al. Enhanced-affinity murine T-cell receptors for tumor/self-antigens can be safe in gene therapy despite surpassing the threshold for thymic selection. Blood. 2013; 122:348–356. [PubMed: 23673862]
33. Chervin AS, Aggen DH, Raseman JM, Kranz DM. Engineering higher affinity T cell receptors using a T cell display system. J Immunol Methods. 2008; 339:175–184. [PubMed: 18854190]
34. Buckler A, Pelletier J, Haber D, Glaser T, Housman D. Isolation, characterization, and expression of the murine Wilms' tumor gene (WT1) during kidney development. Mol Cell Biol. 1991; 11:1707–12. [PubMed: 1671709]
35. Scharnhorst V, van der Eb A, Jochemsen A. WT1 proteins: functions in growth and differentiation. Gene. 2001; 273:141–161. [PubMed: 11595161]
36. Holst J, Vignali K, Burton A, Vignali D. Rapid analysis of T-cell selection in vivo using T cell-receptor retrogenic mice. Nat Methods. 2006; 3:191–197. [PubMed: 16489336]
37. Smith TRF, Verdeil G, Marquardt K, Sherman LA. Contribution of TCR signaling strength to CD8+ T cell peripheral tolerance mechanisms. The Journal of Immunology. 2014; 193:3409–3416. [PubMed: 25156361]
38. Robins HS, et al. Comprehensive assessment of T-cell receptor beta-chain diversity in alphabeta T cells. Blood. 2009; 114:4099–4107. [PubMed: 19706884]
39. Liu B, et al. 2D TCR–pMHC–CD8 kinetics determines T-cell responses in a self-antigen-specific TCR system. European Journal of Immunology. 2014; 44:239–250. [PubMed: 24114747]
40. Huang J, et al. The kinetics of two-dimensional TCR and pMHC interactions determine T-cell responsiveness. Nature. 2010; 464:932–936. [PubMed: 20357766]
41. Holler P, et al. In vitro evolution of a T cell receptor with high affinity for peptide/MHC. Proc Natl Acad Sci U S A. 2000; 97:5387–5392. [PubMed: 10779548]
42. Li Y, et al. Directed evolution of human T-cell receptors with picomolar affinities by phage display. Nat Biotechnol. 2005; 23:349–354. [PubMed: 15723046]
43. Jones LL, Colf LA, Stone JD, Garcia KC, Kranz DM. Distinct CDR3 conformations in TCRs determine the level of cross-reactivity for diverse antigens, but not the docking orientation. The Journal of Immunology. 2008; 181:6255–6264. [PubMed: 18941216]
44. Hunder NN, et al. Treatment of metastatic melanoma with autologous CD4+ T cells against NY-ESO-1. N Engl J Med. 2008; 358:2698–2703. [PubMed: 18565862]
45. Tran E, et al. Cancer immunotherapy based on mutation-specific CD4+ T cells in a patient with epithelial cancer. Science. 2014; 344:641–645. [PubMed: 24812403]
46. Schmitt TM, Stromnes IM, Chapuis AG, Greenberg PD. New Strategies in Engineering T-cell Receptor Gene-Modified T cells to More Effectively Target Malignancies. 2015; 21:5191–5197.
47. Stone JD, Kranz DM. Role of T cell receptor affinity in the efficacy and specificity of adoptive T cell therapies. Front Immunol. 2013; 4:244. [PubMed: 23970885]
48. Mehrotra S, et al. A Co-Receptor Independent Transgenic Human TCR Mediates Anti-Tumor and Anti-Self Immunity in Mice. Journal of immunology (Baltimore, Md: 1950). 2012; 189:1627–1638.
49. Fujiwara H, et al. Antileukemia multifunctionality of CD4(+) T cells genetically engineered by HLA class I-restricted and WT1-specific T-cell receptor gene transfer. Leukemia. 2015; 29:2393–2401. [PubMed: 26104661]
50. Letourneur F, Malissen B. Derivation of a T cell hybridoma variant deprived of functional T cell receptor α and β chain transcripts reveals a nonfunctional α-mRNA of BW5147 origin. European Journal of Immunology. 1989; 19:2269–2274. [PubMed: 2558022]
51. Pui J, et al. Notch1 expression in early lymphopoiesis influences B versus T lineage determination. Immunity. 1999; 11:299–308. [PubMed: 10514008]
52. Brochet X, Lefranc MP, Giudicelli V. IMGT/V-QUEST: the highly customized and integrated system for IG and TR standardized V-J and V-D-J sequence analysis. Nucleic Acids Res. 2008; 36:W503–8. [PubMed: 18503082]
53. Giudicelli V, Brochet X, Lefranc M-P. IMGT/V-QUEST: IMGT Standardized Analysis of the Immunoglobulin (IG) and T Cell Receptor (TR) Nucleotide Sequences. Cold Spring Harb Protoc. 2011 pdb.prot5633–pdb.prot5633.

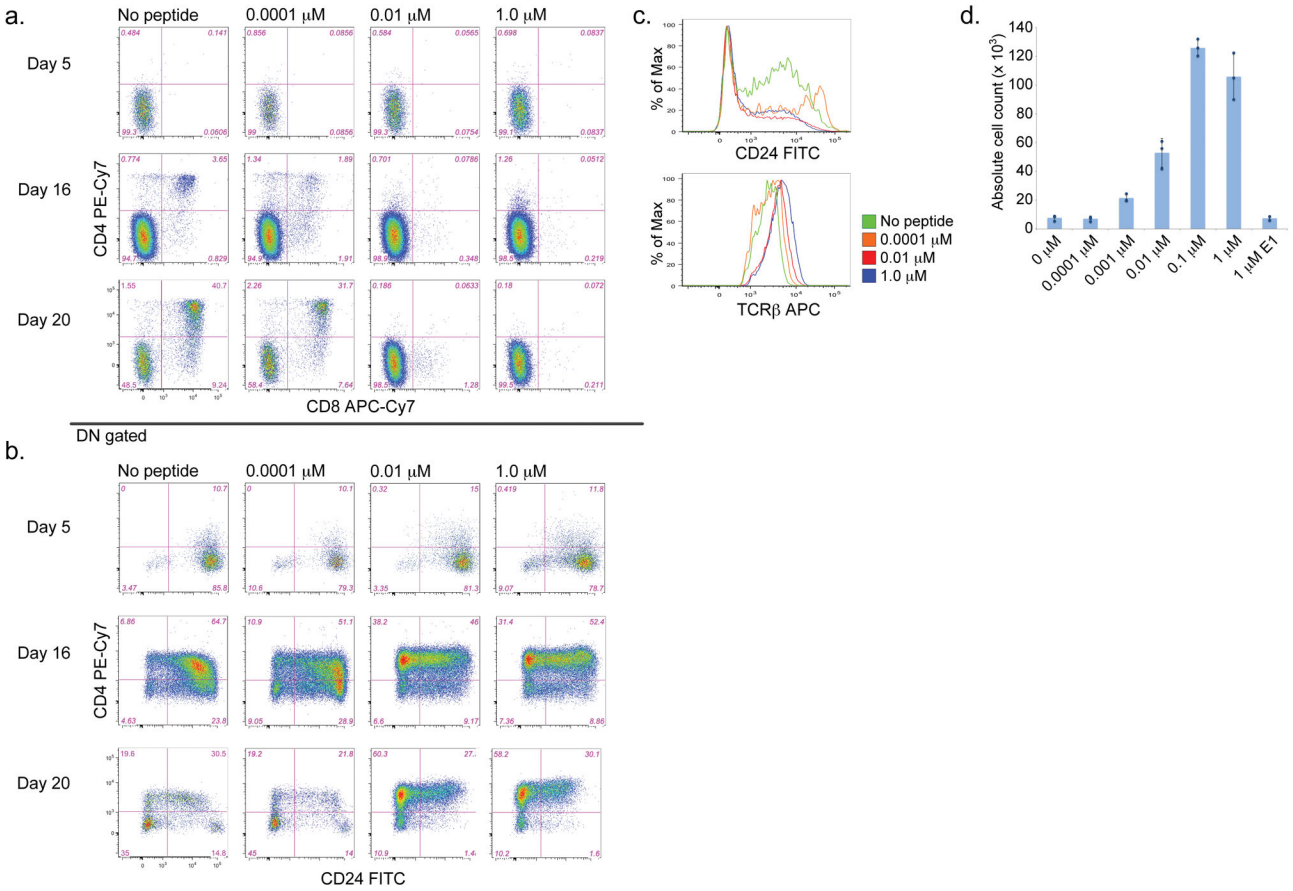

Figure 1. Agonist signaling drives CD4/CD8 DN TCRαβ$^+$ γδ-like T cell development *in vitro*.

(a) DN1 and DN2 Thymocytes were sorted from OT1 mice and cultured on OP9-K^{b}DL1 cells in the presence of titrated concentrations of SIINFEKL peptide on the days indicated. (b) The gated DN cell population was further analyzed for CD24 and TCRβ expression (c) DN TCRβ+ gated cells analyzed for CD24 and TCRβ expression levels. (d) The total number of DN TCRαβ$^+$ cells from day 14 triplicate cultures was calculated for each concentration of added SIINFEKL and for 1 μM of the low affinity, positively selecting peptide EIINFEKL, denoted as E1. Bars indicate the average (± s.d.) of individual data points. Data is representative of 4 independent experiments.

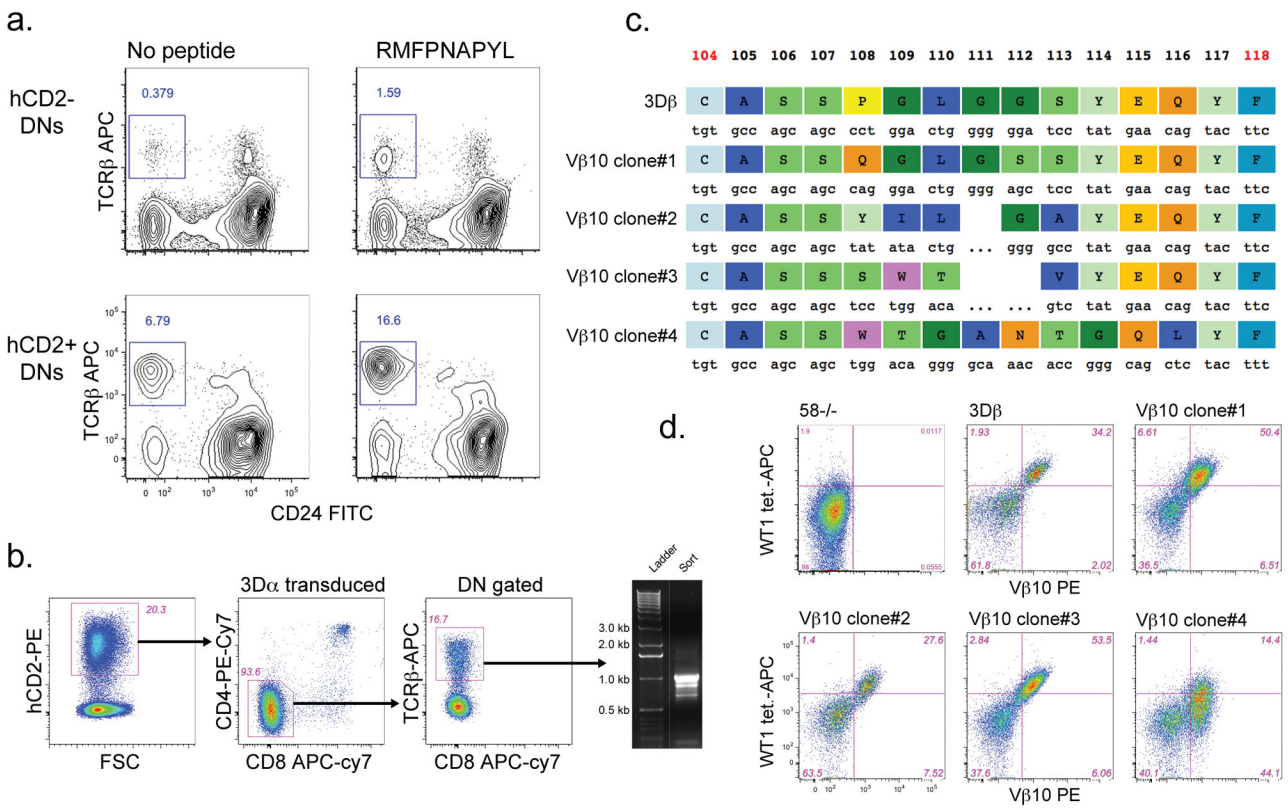

Figure 2. Ectopic expression of an antigen-specific TCRα chain prior to β-selection

DN1 and DN2 progenitor thymocytes were transduced with a retroviral vector containing the TCRα chain of the affinity enhanced WT1-specific TCR (3D-PYY) and hCD2, and cultured on OP9-DL1 cells expressing H-2D^{b} in the presence or absence of 1 μM of WT1 peptide RMFPNAPYL. (a) On day 16 of culture, transduced (hCD2^{+}) and untransduced (hCD2^{-}) cells were gated on CD4^{-}CD8^{-} DN progenitor cells and analyzed for CD24 and TCRβ expression. (b) On day 21, DN TCRαβ^{+} cells were sorted from the 3D-PYYα-transduced population and PCR was performed to amplify Vβ10 TCRβ chains for library construction, and run on an agarose gel with a 1kb DNA ladder. The TCRβ library was transduced into 58$^{-/-}$ cells and TCRβ chains conferring high affinity for WT1 were enriched by cell sorting (Supplementary Fig. 2 and Methods). (c) Isolated TCRβ chains were submitted to IMGT V-Quest[52,53] for sequence analysis for comparison with the parental 3Dβ chain. (d) Four candidate TCRβ chains were detected at high frequency (of 12 unique TCRβ sequences identified in total). These 4 TCRβ constructs were transferred back into MigR1-attR, transduced into CD8^{+}3Dα^{+} 58$^{-/-}$ cells, and assessed for relative tetramer binding.

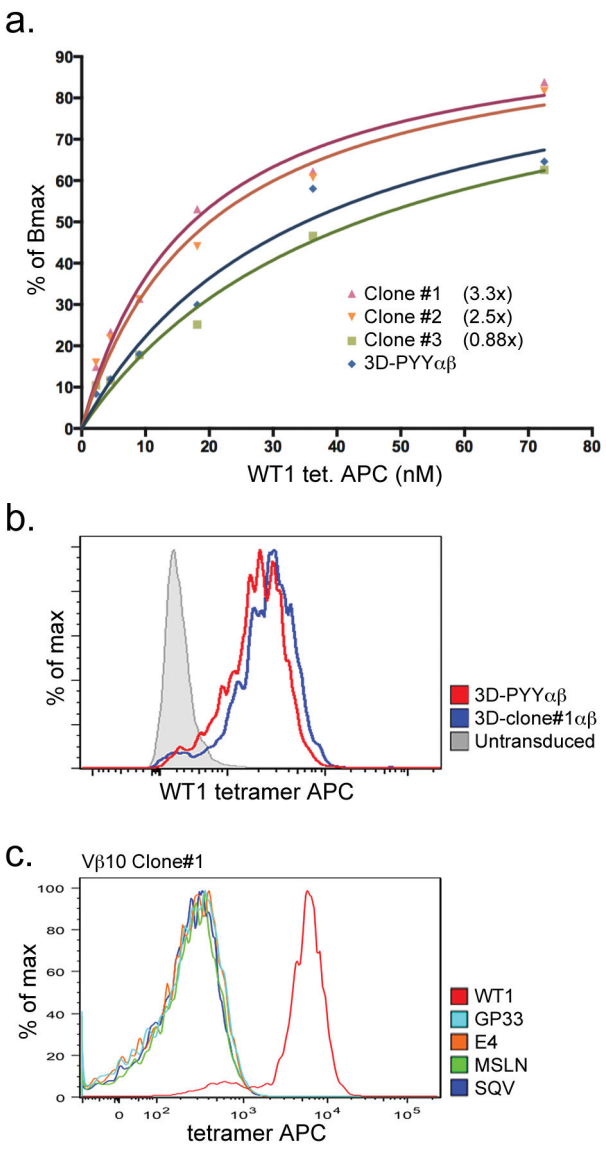

Figure 3. Analysis of enhanced-affinity TCRs recovered from the agonist-selected TCRβ library screen

(a) The relative affinity of the three TCRs exhibiting the highest tetramer binding was determined by staining $58^{-/-}$3D-PYYα cells transduced with the candidate TCRs with titrated amounts of peptide/MHC tetramer and analyzing by flow cytometry. K_D measurements were performed using six 2-fold dilutions of PE-conjugated tetramers, and derived relative K_D values determined from binding curves by non-linear regression, based on the concentration of peptide/MHC tetramer that yielded half-maximal binding. The relative change in derived KD values compared to the parental TCR is listed in parenthesis. (b) The parental Vβ10 TCR and a codon-optimized version of clone#1αβ were transduced into $58^{-/-}$ cells and tetramer binding by cells expressing equivalent levels of Vβ10 TCR was compared. (c) $58^{-/-}$ cells transduced with clone#1αβ paired with 3Dα were stained with WT1 specific tetramer, as well as several non-specific H-$2D^b$ tetramers to assess potential

peptide-independent reactivity towards MHC (GP33: LCMV glycoprotein; E4: Yellow fever virus 17D; MSLN: mouse Mesothelin; SQV: HIV-gag epitope).

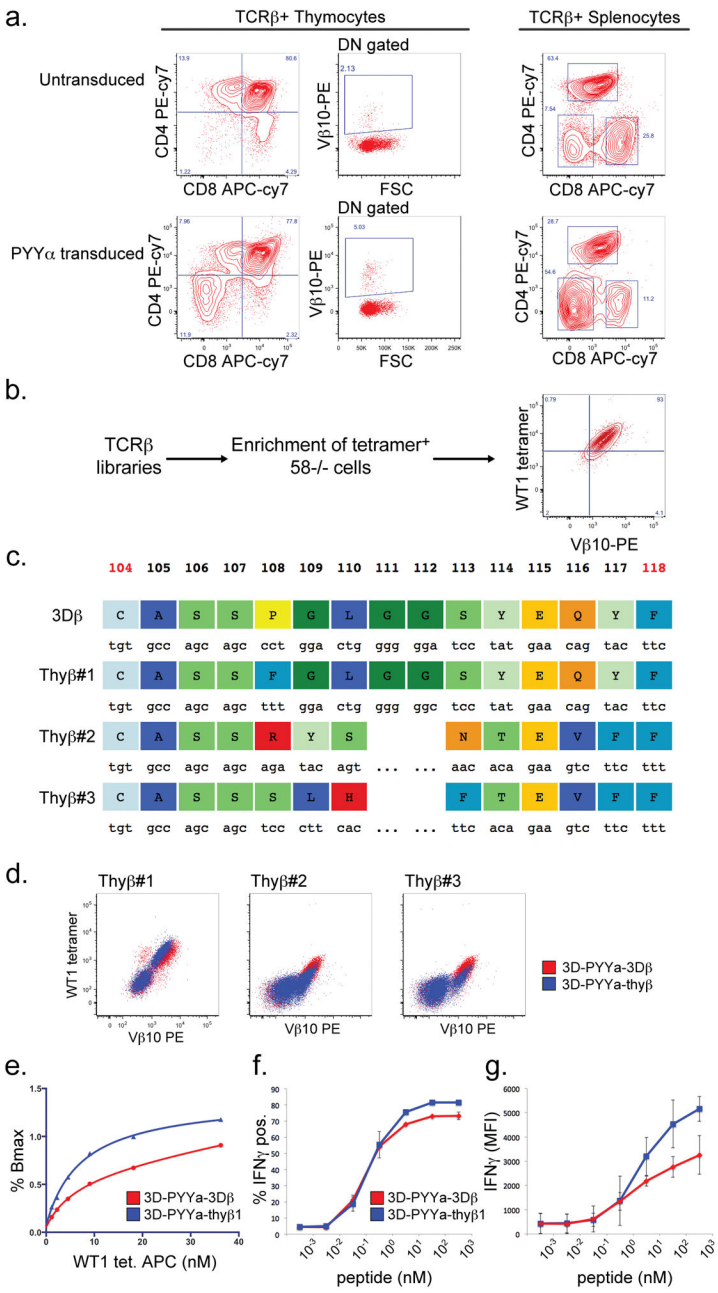

Figure 4. High affinity WT1-specific T cells develop in 3D-PYYα retrogenic mice

BM-derived HPCs were purified from B6 mice, transduced with Mig2-3D-PYYα, and transferred into irradiated B6 recipient mice. (a) Eight weeks after BM transfer, thymus and spleen were analyzed by flow cytometry. Plots are gated on TCRβ$^+$ T cells, which represent ~70% of both untransduced and 3D-PYYα-transduced populations (Data representative of 3 independent experiments with 2, 2, and 4 mice per condition, respectively). (b) Vβ10-restricted TCRβ libraries were generated from the DN TCRαβ$^+$ thymocyte population. Libraries were expressed in 58$^{-/-}$3D-PYYα cells, from which WT1 tetramer$^+$ cells were sorted and expanded. (c) TCRβ chains were recovered from sorted populations and

sequenced. The three most highly enriched TCRβ chains are shown for comparison with the parental 3Dβ. (d) Each of the isolated TCRβ chains were expressed in $58^{-/-}$3D-PYYα cells and analyzed for WT1 tetramer staining relative to Vβ10 expression. Cells expressing candidate library-derived TCRβ chains (blue) are overlaid with those expressing parental 3D PYYα-3Dβ TCR (red). (e) TCR-transduced T cells were stained with titrated concentrations of WT1 tetramer, and MFI values were fit to equilibrium binding curves for 3D-PYYα-Thyβ#1 TCR compared with the parental 3D-PYYα-3Dβ TCR. (f) Peripheral CD8 T cells from $Thy1.1^+$ P14 mice that were transduced to express the 3D-PYYα-3Dβ TCR or the 3D-PYYα-Thyβ#1 TCR were incubated with target cells pulsed with decreasing concentrations WT1 peptide as indicated, and IFNγ producing cells within the $Thy1.1^+$ $CD8^+$ T cell population was assessed. (g) The MFI value for IFNγ staining at each peptide concentration for the experiment shown in (f).

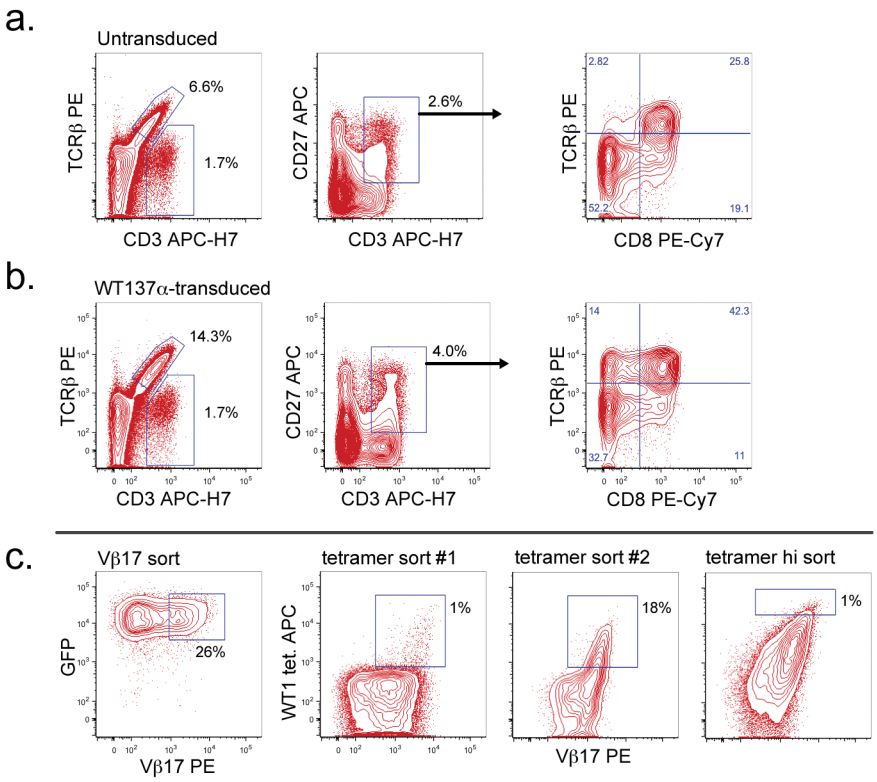

Figure 5. Agonist-selection of *in vitro*-derived human T cells with enhanced affinity for antigen

$CD34^+$ HPCs were purified from umbilical cord blood, lentivirally transduced with $WT1_{37}\alpha$-IRES-GFP and co-cultured with the OP9-A2-DL1 cell line in the presence of 1ug/ml WT1 peptide. (a) untransduced GFP^- or (b) $WT1_{37}\alpha$-expressing GFP^+ cells were analyzed on day 31 of culture for expression of CD3, TCRβ, CD8, and CD27. (c) TCRβ libraries were generated from $CD3^+$ $TCR\beta^+$ $CD27^+$ DN cells as well as $CD3^+$ $TCR\beta^+$ $CD8^+$ cells expressing high levels of CD27 present after day 20 of culture. (c) Cβ1 and Cβ2 libraries were generated using a 5′ Vβ17 primer or (d) using a 5′ universal RACE primer and transduced into H9 cells transduced to express $WT1_{37}\alpha$ (H9.$WT1_{37}\alpha$). H9.$WT1_{37}\alpha$ cells transduced with Vβ17 libraries were first sorted for Vβ17. All library-transduced cells underwent two rounds of low stringency $tetramer^+$ sorts followed by cell expansion, and then sorted for $tetramer^{hi}$ cells from which antigen-specific TCRβ chain genes were cloned for further analysis.

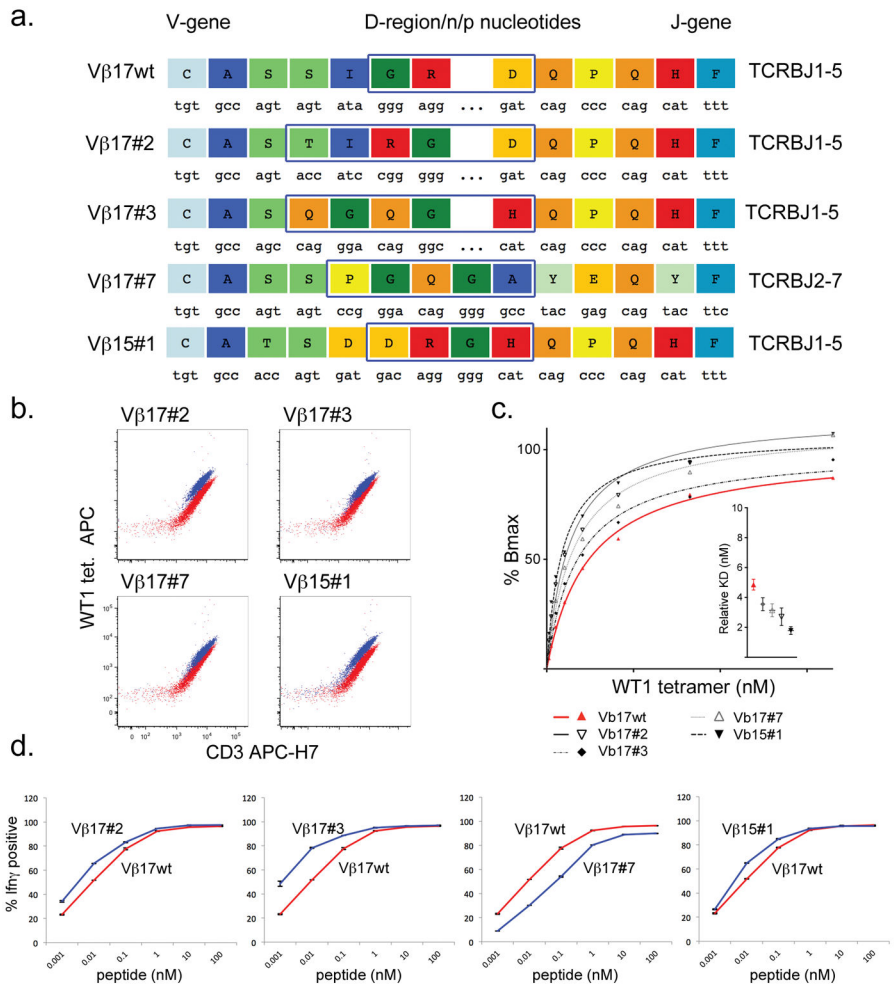

Figure 6. Analysis of human enhanced-affinity TCRs

(a.) Candidate library-derived TCRβ chain CDR3 sequences were submitted to IMGT V-Quest[52,53] for sequence analysis and comparison with the parental Vβ17 *wt* chain. Amino acids predicted to be encoded by the TCRβ D gene segment, or n/p nucleotides are enclosed within the boxed region (b.) Candidate TCRβ chains were coexpressed with $WT1_{37}$α in TCRαβ negative Jurkat76 cells. WT1-specific tetramer staining relative to TCR surface expression for each candidate TCR (red) was compared to the wildtype Vβ17 *wt* TCR (blue). (c.) TCR-transduced T cells were stained with titrated concentrations of WT1 tetramer, and MFI values were fit to equilibrium binding curves, and the derived relative K_D values were calculated by non-linear regression. Error bars represent 95% confidence limits for each calculated K_D value (d.) Human $CD8^+$ T cells were transduced with each of the enhanced affinity TCRs, and sort-purified for tetramer positive cells. Sorted populations were incubated 1:1 with T2 cells alone, or pulsed with titrated concentrations of $WT1_{37}$ peptide, and the percentage of IFNγ producing cells was assessed.